Modeling and Simulation of Branched Wiring Networks

C. Lo and C. Furse

University of Utah,
Department of Electrical and Computer Engineering,
Salt Lake City, Utah, USA
Email: cfurse@ece.utah.edu

Abstract **–** This paper presents a method to analyze the reflectometry responses of a branched network of non-ideal wires. A modified bounce diagram that uses a transition matrix to keep track of signal flow is used. This approach is further improved by including the complex propagation constant to include the frequency dependent filtering effect (phase delay and attenuation) of the non-ideal transmission lines.

I. INTRODUCTION

Modeling and simulation of transmission lines [1-3] has been used to evaluate reflectometry responses or data transmission capability for a variety of applications, particularly evaluation of large scale integrated circuits. With the increasing commercial interest in communication over power lines [4], wire health monitoring for safety and reliability [5], and multipoint communication systems for sensor networks, the ability to perform accurate simulation of transmission responses on branched networks of wires is very important.

A number of approaches for simulating individual point-to-point transmission lines have been developed. Most methods typically rely on the RLGC lumped element model, which models the transmission line as a set of lumped element circuit parameters. Time [6, 7] and frequency domain [8, 9] solutions exist for non-ideal transmission lines including the frequency-dependent losses of the lines. While single lines are of interest in many applications, there are also a number of applications including power distribution systems where the lines branch one or many times, carrying power to multiple locations. Little work has been done on these branched networks. A matrix-based method for analyzing nonideal networks in the time domain was given in [7]. This method works well and could be extended to networks of any size, but it quickly becomes cumbersome and difficult to program for any but the simplest networks. A more scalable method was desired.

This paper introduces a new approach to simulate transmission lines, including easy scalability for branched networks for arbitrary time domain input signals injected at multiple points throughout the network. By merging time domain and frequency domain simulations in a method similar to [6], frequency dependent attenuation on the lossy lines can be taken into consideration for more accurate modeling and simulation. This paper describes the ideal and realistic modeling efforts and how the signatures compare to measured results. The specific application of interest for this paper is the use of reflectometry for location of faults on branched networks of aircraft wiring; however the approach can be readily adapted to other applications.

We will discuss in section II how the transition matrix and state vectors are defined, and present the simulation procedure. The simulation result is compared with measured data in section III. The lumped-element model of the transmission line is the added to the model, and the simulated result is compared with measured data again in section IV.

II. MATRIX REPRESENTATION OF BRANCHED NETWORK

The use of a bounce diagram is a well established method for studying and simulating ideal transmission lines with impedance discontinuities [10]. The bounce diagram is a time domain representation of the reflections in a wire as a set of “bounces” that can be added up to determine the time domain signatures of the signals (reflectometry or communication) on the wire. For transmission lines with multiple branches, the traditional bounce diagram becomes unpalatably complex. Each signal that reaches a branch reflects off the branch and transmits into the branch. To keep track of all of the arms of the branched network, an individual bounce diagram would be needed for each branch, and these separate diagrams would need to be coupled at all of the junction points. In effect, this is what the method described in this paper does. One way to do this is to use a time domain modeling method such as the finite difference time domain method (FDTD) [11], which models the network as an RLGC network, provides special connectivity boundary conditions at all of the junctions, and iteratively evaluates the time domain fields as they move throughout the model. This method works well and provides accurate results, however it is not ideal for use in future work that uses this “forward” model to analyze measured data and produce a “reverse” model of the network that causes them.

In order to provide a simpler method for analysis of the reverse method, a matrix-based approach was used to replace the iterative FDTD method. This is done by subdividing all of the branches of a network into sections of equal length and evaluating the propagation on each segment of the network simultaneously. The term "equal length" means it takes the signal an equal amount of time, T, to travel between adjacent nodes {e.g., x_i and x_j, or x_k and x_l in Fig. 1} where there is an equal distance of z between the adjacent nodes within wire segments. A transition matrix $A = [a_{uv}]$, where u and v are the column and row index, respectively, is used to keep track of the signal flows. The entries of the transition matrix indicate how much of the signal at a particular node in one instant will be redistributed to the other nodes in the following time instant. For a network that has minimal interconnection as shown in Fig. 1, this matrix will be very sparse. A gridded network (which might be used for sensor connectivity) would be less sparse. The column index is the initiating node, and the row index is the receiving nodes.

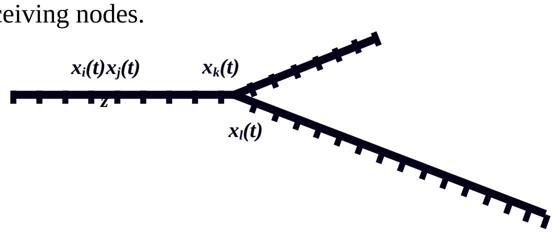

Fig. 1. An example of a simple branched network.

On a transmission line as shown in Fig. 2, the reflection coefficient at any location p on the wire is given by,

$$\Gamma = \frac{V_{ref}}{V_{inc}} = \frac{Z_1 - Z_0}{Z_1 + Z_0} \tag{1}$$

and the transmission coefficient is given by,

$$T = 1 + \Gamma = \frac{V_{trans}}{V_{inc}} \tag{2}$$

where V_{inc} is the incident voltage, V_{ref} is the reflected voltage, V_{trans} is the transmitted voltage, Z_0 and Z_1 are the impedance of the transmission line before and after the point p.

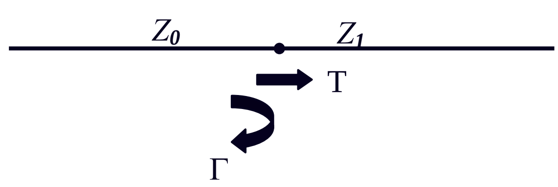

Fig. 2. Illustration of transmission and reflection coefficients.

When the impedances are equal at adjacent notes, such as x_i and x_j shown in Fig. 1, the reflection coefficient is 0, and the transmission coefficient is 1. When a junction between two wires of equal impedance Z_0 is encountered, their effective impedance is $Z_0/2$, the reflection coefficient is 1/3, and the transmission coefficient is 2/3. This means for a network as in Fig. 1, we will have $a_{ij} = 1$, $a_{kl} = 2/3$, etc.

At time t, the signal containing the reflections from all of the nodes can be presented as a state vector x_t where the signal at all of the nodes at time t can be found from the signal at the previous time t-T,

$$\overline{x}_t = A\overline{x}_{t-T}\ . \tag{3}$$

This method is iterative from time step to time step, and is therefore well suited for evaluation of a reflectometry signature, which is normally represented in the time domain. The method is simpler and faster than the FDTD method, and can be adapted to include the effects of frequency dependent attenuation that is present on all realistic wiring systems as described in the following section.

III. COMPARISON OF SIMULATED AND MEASURED DATA

Figure 3 shows a branched network that is simulated with this method (ideal case) and compared with its measured time domain reflectometry (TDR) signature for realistic (slightly lossy, RG58 coax) wire. A TDR transmits a fast rise time step function down the wire and records its reflections in the time domain. The location and change in impedance along the wire are determined from the observation of the delay and the magnitude of the reflection.

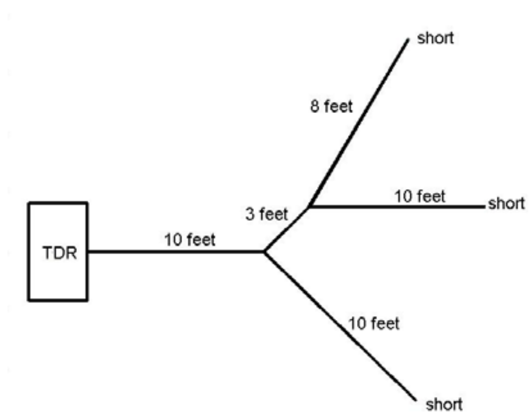

Fig. 3. Branched network to be simulated and measured with TDR. The cables are 50 ohm RG58 coaxial cable.

IV. LUMPED-ELEMENT MODEL OF TRANSMISSION LINE

We can see from Fig. 4 that the simulation is close to the measured response, but it misses the frequency dependent filtering effect of the lossy transmission line. Many transmission lines are much lossier than this coaxial cable and as a result have a much greater mismatch between ideal and measured data. This attenuation is frequency-dependent and can be added to the model by including RLGC transmission line parameters [10].

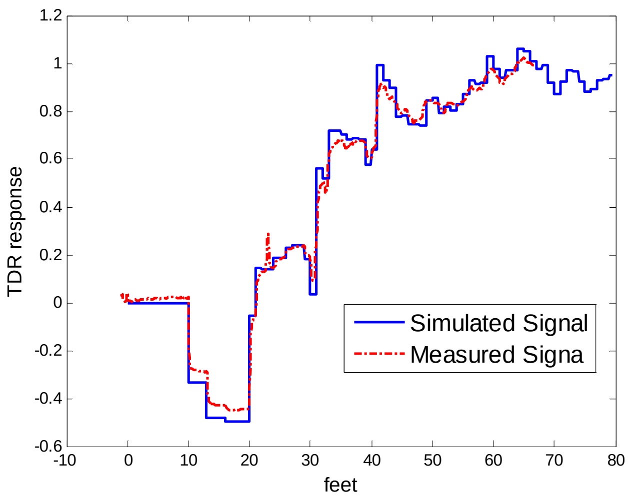

Fig. 4. Comparison of simulated and measured TDR responses for the network of wires shown in Fig. 2.

In equation (4) R is the resistance of the conductor, which is typically small; however, G is the conductance in the insulation and the region around an unshielded transmission line which is typically not small for the high frequency terms in the TDR step function. The complex propagation constant describes the attenuation (real part) and phase shift (imaginary part) for a transmission line,

$$\gamma(\omega) = \sqrt{(R + j\omega L)(G + j\omega C)}\ . \tag{4}$$

This propagation can be considered to be a filter with a transfer function of,

$$H(\omega) = e^{-\gamma(\omega)z}\ . \tag{5}$$

Because it now involves a filtering effect, the signal contained in at a node is now no longer single valued but is a vector of signal values in time at each individual node as shown in Fig. 5.

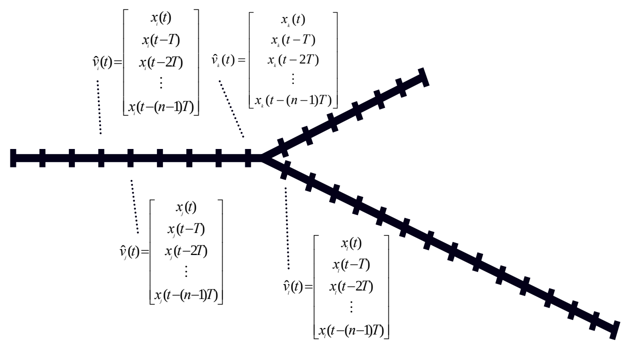

Fig. 5. Illustration of signal vectors, where $x_i(t)$, $x_j(t)$, $x_k(t)$ and $x_l(t)$ are as represented in Fig. 1.

The sampling interval or time resolution for the simulation is naturally determined by the distance z between the adjacent nodes, i.e. the time it takes for the signal to travel a distance of z that is T as in equation (1). According to sampling theory, this sampling interval determines the highest frequency contained in our simulation. At the same time, the frequency resolution, $\Delta\omega$, of the simulation is determined by the length of the signal vectors at individual nodes.

Let the length of the signal vectors be n, and the highest simulation frequency be Ω, which gives the following relationships,

$$\Omega = n\Delta\omega = \frac{2}{T} \tag{6}$$

and

$$nT = \frac{2}{\Delta\omega}\ . \tag{7}$$

The discrete form of the filter $H(\omega)$ becomes

$$H = \begin{bmatrix} 1 &&&&&&& \\ & e^{-\Delta\omega z} &&&&&& \\ && e^{-2\Delta\omega z} &&&&& \\ &&& \ddots &&&& \\ &&&& e^{-\Omega z} &&& \\ &&&&& e^{(n-1)\Delta\omega z} && \\ &&&&&& \ddots & \\ &&&&&&& e^{\Delta\omega z} \end{bmatrix}. \tag{8}$$

To illustrate the signal vectors at adjacent nodes, we assume $H = I$, i.e., the transmission line is a perfect conductor, or the response of the branched network is an impulse. Then, as in equation (8), we may have at time t,

$$\hat{v}_i(t) = \begin{bmatrix} x_i(t) \\ x_i(t-T) \\ x_i(t-2T) \\ \vdots \\ x_i(t-(n-1)T) \end{bmatrix} \quad (9)$$

and

$$\hat{v}_j(t) = \begin{bmatrix} x_j(t) \\ x_j(t-T) \\ x_j(t-2T) \\ \vdots \\ x_j(t-(n-1)T) \end{bmatrix}. \quad (10)$$

As $H = I$, we have,

$$v_j(t) = \hat{v}_i(t-T). \quad (11)$$

In fact, when H is flat in the frequency domain, there is no information gained by keeping the higher frequency resolution. So, we can set $n = 1$, and when we apply the argument of equation (11) to all the other nodes, we will have equation (3), just as it should be.

Now, let the Fourier Transform of $\hat{v}_i(t)$ and $\hat{v}_j(t)$ be $\hat{V}_i(t)$ and $\hat{V}_j(t)$, respectively. Then for a transmission line with H as in equation (4),

$$\hat{V}_j(t) = H\hat{V}_i(t-T) \quad . \quad (12)$$

For this application, it is easier to apply this in the frequency domain rather than in the time domain.

We can further compact our notation by combining the signal vectors at individual nodes into a state vector where each of its entries is a vector itself. The state vector is defined as,

$$\overline{V}_t = \begin{bmatrix} \hat{V}_1^T(t) \\ \hat{V}_2^T(t) \\ \vdots \\ \hat{V}_i^T(t) \\ \hat{V}_j^T(t) \\ \vdots \end{bmatrix} \quad (13)$$

where T indicates a vector transpose.

A is the transition matrix telling us the transition properties between the adjacent nodes, and it can be applied to the frequency domain as well. We have to be aware that the entries of A are now applied to the entries of the state, which are vectors. Combining equations (3), (12), and (13) we have,

$$\overline{V}_t = AH\overline{V}_{t-T} \quad (14)$$

The simulated TDR response of RG58 cables in the branched structure shown in Fig. 3 is presented in Fig. 6.

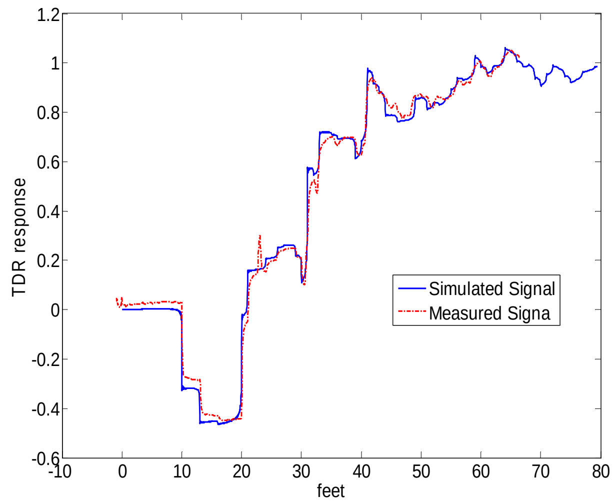

Fig. 6. Comparison of simulated response with transmission line model added and measured TDR response.

From Fig. 6, we observe that by adding the complex propagation constant, the simulation result is improved. Additional differences between the simulated and measured system may be due to variation between the ideal and actual characteristic impedance of the cable and impedance of the connections that was not accounted for in the model.

V. HIGH SPEED REALIZATION

Implementation of equation (14) can be further speeded up if the network consists of a uniform wire type, and the TDR input signal is used as in the previous examples.

Some basic mathematical properties can be used to facilitate further discussion. Let the network be represented by transfer function $h(\cdot)$, which is linear. Then an input signal $f(\cdot)$ will generate an output response of $y(t) = h * f(t)$. In the above expression, * indicates the convolution operation which is defined as,

$$\begin{aligned} y(t) &= h * f(t) \\ &= \int h(\tau) f(t-\tau) d\tau. \end{aligned} \quad (15)$$

This may be represented graphically as in Fig. 7.

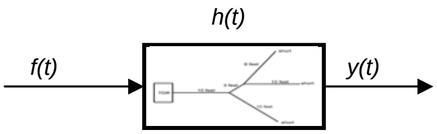

Fig. 7. System representation of wire network.

From equation (15), we have,

$$\begin{aligned} \frac{d}{dt} h * f(t) &= \frac{d}{dt} \int h(\tau) f(t-\tau) d\tau \\ &= \int h(\tau) \frac{d}{dt} [f(t-\tau)] d\tau \\ &= \int h(\tau) f'(t-\tau) d\tau \\ &= h * f'(t) \\ \Rightarrow \quad h * f(t) &= h * f'(t) dt \quad . \end{aligned} \tag{16}$$

Since the TDR signal, *f(t)*, is a step function at *0*, then *f'(t)* becomes a delta function *δ(t)*. Then, from equation (3) without considering the filtering effect, the impulse response of the wire network in Fig. 3 is a train of impulses with peaks corresponding to junctions of impedance mismatches and their multiple reflections. Figure 8 shows this train of impulses.

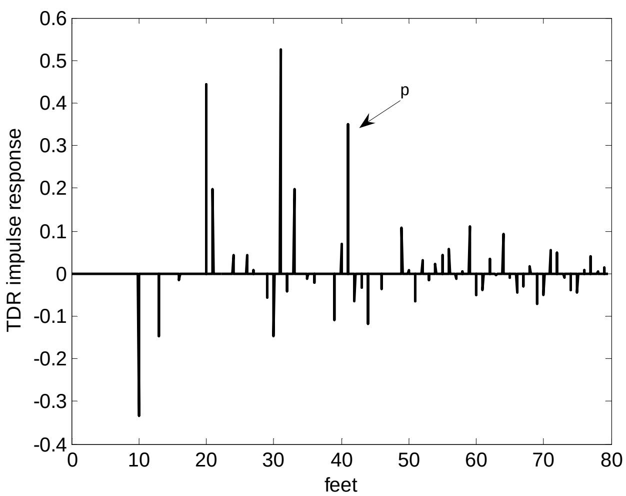

Fig. 8. Impulse response of the wire network in Fig. 3.

Considering a particular peak, p_k, from the train of impulses as marked in Fig. 6, which has a magnitude of A_k and a time delay of T_k gives,

$$p_k = A_k \delta(t - T_k)\,. \tag{17}$$

There are two important aspects of this derivation. First, since n(t) is linear, the filtering effect of the wire can be considered for independent peaks. Second, no matter how many junctions cause multiple reflections of p_k, the total distance of its travel can be determined by delay T_k . The filtering effect p_k will experience depends only on the length of wire it travels through. This filter is denoted by $h_{T_k}(t)$, and the filtered version, of p_k becomes,

$$p_k = A_k h_{T_k}\left(t - T_k\right). \tag{18}$$

Summarizing the above two aspects, we have,

$$y'(t) = \sum_i A_i h_{T_i}(t - T_i)\,. \tag{19}$$

In its discrete version, equation (19) becomes,

$$y'[n] = \sum_i A_i h_{m_i}[n - m_i] \tag{20}$$

where the sample rate is the same as in equations (6) and (7), and m_i is the number of samples for the signal to travel in T_i. So from equation (8), the Fourier transform of $h_{m_i}[n - m_i]$ becomes,

$$H_{m_i} = \Lambda (He)^{m_i} \tag{21}$$

where

$$\Lambda = \begin{bmatrix} 1 & & & & & & & \\ & e^{-j2\pi\Delta\omega} & & & & & & \\ & & e^{-j4\pi\Delta\omega} & & & & & \\ & & & \ddots & & & & \\ & & & & e^{-j2\pi\Omega} & & & \\ & & & & & e^{j2\pi(n-1)\Delta\omega} & & \\ & & & & & & \ddots & \\ & & & & & & & e^{j2\pi\Delta\omega} \end{bmatrix}.$$

Then equation (19) may be written as,

$$Y'[k] = \Lambda \sum_i A_i (eH)^{m_i} \bar{1} \tag{22}$$

where $\bar{1}$ is a unit vector. Then y'[n] is found from the inverse Fourier transform of equation (22). Then from equation (16), y[n] can be obtained by integration. Figure 9 shows the filtered impulse response of the wire network in Fig. 3 with equation (22), and its integral. The integral y[n] is the same as the result shown in Fig. 6.

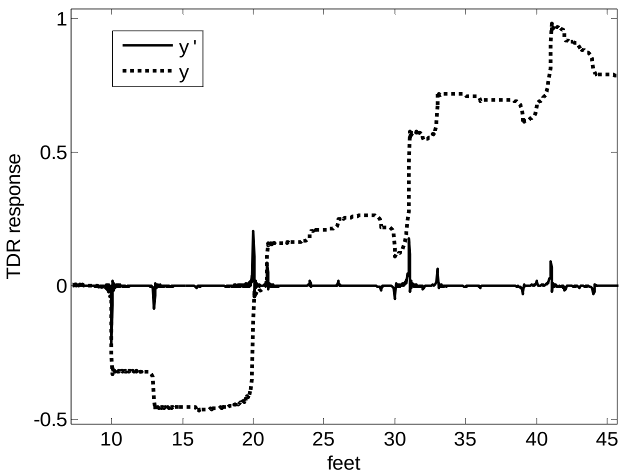

Fig. 9. Impulse response of the wire network in Fig. 3 filtered as equation (24) and its integral.

VI. CONCLUSION

This paper has described a simple and effective method of analyzing time domain fields on ideal or non-ideal branched networks of wires. The method can be used to evaluate both reflectometry signatures and communication systems made up of branched wire networks. It could also be adapted to a grid of wires such as may be used in interconnected sensor networks. Use of the frequency-dependent attenuation constant provided significantly better agreement between the ideal and measured responses.

REFERENCES

[1] L. N. Drowsy, *Modern Transmission Line Theory and Applications*, John Wiley and Sons, Inc., 1997.

[2] C. R. Paul and R. J. W. McKnight, "Prediction of crosstalk involving twisted pairs of wires – Part I: A transmission line model for twisted-wire pairs," *IEEE Trans. On EMC*, vol. 21, no. 2, May 1979.

[3] T. Bostoen, P. Boets, M. Zekri, L. Van Biesen, T. Pollet, and D. Rabijins, "Estimation of the transfer function of a subscriber loop by means of a one-port scattering parameter measurement at the central office," *IEEE Journal on Selected Areas in Communications*, vol. 20, no. 5, June 2002.

[4] P. Lots, Powerline communications, in Proc. TI KVIV Workshop on the use of powerlines for non-power applications, Antwerpen, Belgium, December 9, 1998.

[5] C. Lo and C. Furse, "Noise domain reflectometry for wire fault location," *IEEE Trans. EMC*, February 2005.

[6] J.-F. Mao and Z.-F. Li, "Analysis of the time response of multiconducctor transmission lines with frequency-dependent losses by the method of convolution-characteristics," *IEEE Trans. MTT*, vol. 40, no. 4, pp. 637-644, April 1992.

[7] A. Djordjevic and T. K. Sarkar, "Anlaysis of time response of l ossy multiconductor transmission line networks," *IEEE Trans. MTT*, vol. 35, no. 10, pp. 898-908, October 1987.

[8] G. Antonini, G. Ferri, "A new approach for closed-form transient analysis of multiconductor transmission lines," *IEEE Trans. EMC*, vol. 46, no. 4, pp. 529-543, November 2004.

[9] L. Gruner, "Multiconductor transmission lines and the Green's matrix," *IEEE Trans. MTT*, pp. 837-839, Septemper 1974.

[10] F. T. Ulaby, *Fundamentals of Applied Electromagnetics*, Prentice Hall, 2004.

[11] R. Parakh, "The invisible fray: A formal assessment of the ability of reflectometry to locate frays on aircraft wiring," *Master's thesis*, University of Utah, Salt Lake City, Utah, 2004.